*Acta Cryst.* (1999). B**55**, 543–553

# Modelling the crystal structure of the 2-hydronitronylnitroxide radical (HNN): observed and computer-generated polymorphs

G. Filippini,[a]* A. Gavezzotti[b] and J. J. Novoa[c]

[a]*Centro CNR per lo Studio delle Relazioni tra Struttura e Reattività Chimica, Università di Milano, Milano, Italy,* [b]*Dipartimento di Chimica Strutturale e Stereochimica Inorganica, Università di Milano, Milano, Italy, and* [c]*Dipartament de Química Física, Facultat de Química, Universitat de Barcelona, Barcelona, Spain.*
*E-mail: fili@rs6.csrsrc.mi.cnr.it*

(*Received 11 December 1998; accepted 22 January 1999*)

## Abstract

The crystal structures of two polymorphs of 4,4,5,5-tetramethyl-4,5-dihydro-1*H*-imidazol-1-oxyl 3-oxide (the 2-hydronitronylnitroxide radical, HNN) are analyzed by packing energy criteria. Other unobserved polymorphic crystal structures are generated using a polymorph predictor package and three different force fields, one of which is without explicit Coulomb-type terms. The relative importance of several structural motifs (hydrogen-bonded dimers, shape-interlocking dimers or extended hydrogen-bonded chains) is discussed. As usual, many crystal structures within a narrow energy range are generated by the polymorph predictor, confirming that *ab initio* crystal-structure prediction is still problematic. Comparisons of powder patterns generated from the atomic coordinates of the X-ray structure and from computational crystal structures confirm that although the energy ranking depends on the force field used, the X-ray structure of the $\alpha$ polymorph was found to be among the most stable ones produced by the polymorph predictor, even using the chargeless force field.

## 1. Introduction

A proper prediction of the possible crystal structures of a molecular magnet has never been presented before. As a first approach, in this work we address this problem with the simplest molecular magnet of the $\alpha$-nitronyl nitroxide family, the HNN radical (Fig. 1). This family of compounds has many members which are known to present remarkable magnetic properties, in some cases even bulk ferromagnetism (Gatteschi *et al.*, 1991; Miller & Epstein, 1994; Kinoshita, 1994; Itoh *et al.*, 1997). The prediction of HNN polymorphs is an interesting problem which is relevant to magnetic molecular materials. The two NO groups show localized net charges which create a strong molecular dipole, calculated to be 3.872 D (Deumal *et al.*, 1997), and make them good hydrogen-bond acceptor groups for C($sp^2$)—H···O and C($sp^3$)—H···O bonds. Previous *ab initio* computations (Deumal *et al.*, 1997) have shown that the strength of the first type of bond is much larger than that of the second (−15.5 *versus* −1.6 kJ mol$^{-1}$). The NO groups have positive spin densities, while negative spin densities are located on the $sp^2$ C atom (Novoa & Deumal, 1997). The relative orientation of the two NO groups in the crystal is commonly associated with the magnetic properties of these materials (Hosokoshi, Tamura, Nozawa, Suzuki, Sawa *et al.*, 1995). Since magnetism depends on the details of the molecular arrangement in the solid (Takeda *et al.*, 1998; Miller & Epstein, 1994; Kahn, 1993), an understanding, prediction, and eventually control of the crystal structure by theoretical methods would be highly desirable. We report here a quantitative energetic analysis of the observed polymorphs of crystalline HNN, the computer generation of hypothetical crystal structures for this compound by polymorph-predictor computer protocols, and, finally, attempted predictions of its possible crystal structures. Since it might be thought that a specialized force field would be required to describe intermolecular interactions in this radical compound, the development and validation of force fields for this kind of molecular and crystalline system are discussed with special regard to the calculation of electrostatic contributions.

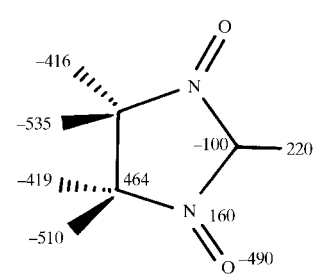


Fig. 1. Point-charge parameters (e × 10$^3$) for 6-exp-1 calculations. Methyl H-atom charges range from +0.1 to +0.16 e.

## 2. Crystal potentials and computational details

Lattice energies for HNN polymorphs were calculated using empirical potentials of the 6-exp or 6-exp-1 form, *i.e.* where the atom *i*–atom *j* potential energy is given by $E_{ij} = A\exp(-BR_{ij}) - CR_{ij}^{-6}$ or $E_{ij} = A\exp(-BR_{ij}) - CR_{ij}^{-6} + q_iq_jR^{-1}$, respectively. $A$, $B$ and $C$ are empirical parameters and the $q$'s are adjustable atomic site charge parameters. The lattice energies of the observed polymorphs were calculated on the basis of the crystallographic atomic coordinates, but the crystal structures were also energy-optimized with respect to lattice parameters and rigid-body molecular positional parameters using the *PCK* procedure (Williams, 1983). An ideally perfect potential should produce no relaxation, except for a small cell shrinkage owing to the fact that potential energy calculations do not include the effect of thermal vibrations. Computational polymorphs were generated by the *PROMET* procedure (Gavezzotti, 1997), which consists of three main steps: (i) a search of the potential energy hypersurface for molecular pairs or clusters built around symmetry elements; (ii) a search of the crystal structures that can be generated from these progenial clusters; and (iii) from these approximate crystal structures, a final optimization stage also using *PCK*. Stage (i) uses only 6-exp potentials, stage (ii) also only uses 6-exp potentials, for speed, while stage (iii) uses 6-exp-1 potentials and the Ewald method to force convergence of lattice sums over Coulomb-type terms (Williams, 1983). Furthermore, it ensures that the Hessian is positive definite, and, therefore, that the structure is in a true energy minimum with the only constraint being the chosen space-group symmetry.

While 6-exp potentials for general organic compounds with conventional hydrogen bonds are available (Filippini & Gavezzotti, 1993; Gavezzotti & Filippini, 1994), there is no accepted set of potential energy functions of empirical origin for potentially relevant interactions in the system under consideration here, namely C($sp^2$)—H···O═N and C($sp^3$)—H···O interactions. Therefore, the problem of the parametrization of these interactions arises. For C($sp^2$)—H···O═N, as a first approximation, the empirical 6-exp potentials developed for the nitro–amino N═O···H—N hydrogen bond (Filippini & Gavezzotti, 1994) were used; this scheme is called SET1 ($A$ = 5.502 × $10^6$, $B$ = 7.78, $C$ = 363, $R^0$ = 1.80 Å, $\varepsilon$ = 6.11). A chemically more reasonable approximation was thought to be an average (geometrical for $A$ and $C$, arithmetic for $B$) of these potentials and those for the purely dispersive C—H···O interaction (Filippini & Gavezzotti, 1993); this scheme is called SET2 ($A$ = 1.275 × $10^6$, $B$ = 6.30, $C$ = 399, $R^0$ = 2.13 Å, $\varepsilon$ = 2.38). The equilibrium distance in SET1 potentials is clearly at a very short interatomic separation; that for SET2 looks more adequate. No special parametrization was introduced for the weaker C($sp^3$)—H···O interactions.

However, previous experience (Bürgi *et al.*, 1974; Gavezzotti, 1991) shows that in small molecules containing more than one carboxyl group (anhydrides, polyketones) a subtle balance between H···O and C···O interactions is established. Often, crystals of such highly polar molecules cannot be safely treated without the introduction of charge parameters and Coulombic terms (Gavezzotti & Filippini, 1994), corresponding to the 6-exp-1 potential.

The introduction of Coulombic terms in the lattice summations obscures the discussion of local effects, since the total Coulomb-type interaction energy results from contributions which are very diffuse in space, and its value may oscillate widely as a function of cutoff. Thus, by definition, these contributions to the overall lattice stabilization [or destabilization, since there are cases, like hexachlorobenzene (Bates & Busing, 1974), where the Coulomb-type contributions are calculated to be net-destabilizing] are such that inferences on energies or forces over atomic pair interactions are unwarranted.

An estimate of the point-charge parameters needed for the calculations was obtained by a molecular-orbital calculation according to the Merz–Singh–Kollman scheme (Besler *et al.*, 1990) to reproduce the electrostatic potential obtained from an MP2/6-31G(2*d*,2*p*) computation (Frisch *et al.*, 1995). In the following, we will refer to SET1 calculations (SET1 parameters without point charges), SET1Q calculations (SET1 parameters plus charges), or SET2Q calculations (SET2 parameters plus charges), it being understood that Coulomb-type terms are introduced only when overall crystal-structure optimization is performed, that is, in the relaxation of observed structures in *PROMET* stage (iii) (see above).

H-atom positions were always renormalized to a C—H distance of 1.08 Å, a vital requirement (Filippini & Gavezzotti, 1993; Gavezzotti & Filippini, 1994) whenever organic crystal-packing geometries or energies are discussed. A 10 Å cutoff was applied in all lattice-energy summations, except of course for Coulomb-type terms, for which the Ewald method was used.

## 3. The crystal packing of HNN

The composition of the molecular coordination sphere in a crystal structure may be described using the concept of structure determinants (Gavezzotti & Filippini, 1994). A reference molecule having been chosen, each determinant identifies a molecule in its coordination sphere by (i) a symmetry operator, by which it is related to the reference molecule, (ii) a distance from its centre of mass to that of the reference molecule, and (iii) an interaction energy with the reference molecule (as explained previously, in the calculation of this energy Coulomb-type terms are omitted.) Owing to these and other approximations, here interaction energies are to

Table 1. *X-ray and relaxed (after the PCK procedure) crystal structures of HNN*

| | $a$ (Å) | $b$ (Å) | $c$ (Å) | $\beta$ (°) | Density (g cm$^{-3}$) | −PE (kJ mol$^{-1}$) | $V_{cell}$ (Å$^3$) |
|---|---|---|---|---|---|---|---|
| $\alpha$; $P2_1/c$, $Z = 4$ | | | | | | | |
| X-ray | 6.332 (2) | 11.611 (2) | 11.983 (3) | 106.29 (2) | 1.23 | — | 845.6 |
| SET1 | 6.17 | 11.46 | 11.72 | 105.6 | 1.31 | 86.1 | 798.2 |
| SET1Q | 6.25 | 11.58 | 11.88 | 104.7 | 1.25 | 124.7 | 831.7 |
| SET2Q | 6.17 | 11.34 | 11.64 | 105.1 | 1.33 | 123.1 | 786.3 |
| $\beta$; $P2_1/c$, $Z = 16$ | | | | | | | |
| X-ray | 12.133 (2) | 14.080 (3) | 19.991 (4) | 92.96 | 1.22 | 78.9 | 3410.6 |
| SET1 | 11.827 | 13.963 | 19.370 | 92.37 | 1.30 | 84.0 | 3205.8 |

be considered as guidelines, rather than strictly quantitative indicators, of molecule–molecule cohesive strength. The distance between centres of mass is a more objective criterion, since nearest neighbours are usually strongly interacting neighbours. Owing to crystal symmetry, any molecule can be chosen as the reference one.

### 3.1. *The α-HNN polymorph*

Results of the lattice-energy optimization procedure for the $\alpha$-polymorph of HNN (Hosokoshi, Tamura, Nozawa, Suzuki, Kinoshita *et al.*, 1995) are shown in Table 1. All three parameter sets produce just minor distortions of the observed structure, an encouraging result (see §2). Even the chargeless parameter set seems adequate in this respect. Lattice energies calculated with 6-exp-1 parameter sets are larger, owing to a net stabilizing Coulomb-type contribution of about 38 kJ mol$^{-1}$. No quantitative assessment of these results is possible, since the sublimation enthalpy of HNN is not available.

The structure determinants of $\alpha$-HNN are shown in Table 2. The main structure determinant (the closest molecule in the coordination sphere) is a molecule related by a centre of inversion, forming a close-packed, interlocking dimer (the *AB* pair in Fig. 2), labelled as DIM1. Pairs of molecules related by translation along the short cell axis provide about as much cohesive energy, and the same applies to pairs of molecules related by screw or glide operators. The C—H···O hydrogen-bonded dimer (labelled HB, the *AC* pair in Fig. 2) ranks third in this list of closest neighbours. Remarkably, the DIM1 dimer offers a chance for juxtaposition of molecular dipoles with opposite direction, sometimes invoked as stabilizing in crystal packing. In any case, the coordination sphere of $\alpha$-HNN is scattered, with many molecules at about the same distance from the reference one, as expected for such a small molecule of nearly globular shape.

The X-ray H···O distance, about 2.34 Å, indicates a rather strong C—H···O hydrogen bond. Molecular-orbital calculations (Deumal *et al.*, 1997) provide an interaction energy of −23 kJ mol$^{-1}$ for the dimer of a model molecule. The overall SET2 dimer 6-exp cohesive energy, −13 kJ mol$^{-1}$, is at least of the correct order of magnitude.

### 3.2. *The β-HNN polymorph*

The $\beta$ phase of HNN (Hosokoshi, 1995), $P2_1/c$, $Z = 16$, has four molecules in the asymmetric unit. The concept of structure determinant loses some of its meaning for structures with more than one molecule in the asymmetric unit; however, the same basic structural motifs of the $\alpha$ phase, namely the DIM1 and the HB dimers, are present (Fig. 3), although with a rather substantial geometrical deformation. In addition, this phase shows a catemer hydrogen-bonding motif of an infinite ribbon of hydrogen bonds. The generation or prediction of crystal structures with two (let alone four) molecules in the asymmetric unit would be typically outside the capabilities of crystal-structure generation methods, so the $\beta$ phase will not be considered further here. The fact that an irreversible transition to the $\beta$ phase occurs at 333 K (Deumal *et al.*, 1997) suggests that the $\beta$ phase is metastable at room temperature.

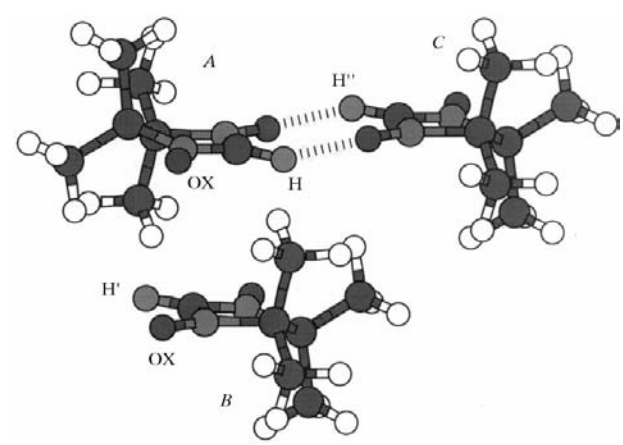


Fig. 2. The main structure determinants in $\alpha$-HNN (Tables 2 and 4). The corresponding views of the X-ray structure, H74, H20 and H58 are nearly identical. Detailed geometries (in the order X-ray, H74, H58, H20): vertical OX···OX 3.80, 3.84, 4.06, 3.97 Å; diagonal H···H′ 4.09, 4.12, 4.49, 4.36 Å; diagonal H′···H″ 6.33, 6.38, 6.26, 6.23 Å. *A*–*B* pairs: DIM1 dimer; *A*–*C* pairs: HB dimer.

Table 2. *Structure determinants and relevant geometrical data (Å, °) for experimental and calculated crystal structures*

Each structure determinant comprises a symmetry operator symbol (I inversion centre, S screw, G glide, T translation), a distance between centres of mass and an interaction energy (kJ mol$^{-1}$). Labels are as in Tables 3–5.

| α-HNN† | | | H74 (SET2Q) | | | H58 (SET1Q) | | | H20 (SET1) | | |
|---|---|---|---|---|---|---|---|---|---|---|---|
| I | 5.2 | −26 | I | 5.1 | −26 | I | 5.1 | −25 | I | 5.1 | −25 |
| 2 × T | 6.3 | −14 | 2 × T | 6.4 | −13 | I | 6.2 | −12 | 2 × T | 6.2 | −15 |
| I | 6.7 | −13 | I | 6.4 | −11 | 2 × T | 6.3 | −14 | I | 6.3 | −17 |
| 2 × S | 6.7 | −11 | 2 × S | 6.6 | −13 | 2 × G | 6.3 | −16 | 2 × G | 6.4 | −16 |
| 2 × G | 6.8 | −13 | 2 × G | 6.8 | −11 | 2 × S | 6.8 | −13 | 2 × S | 6.9 | −13 |
| 2 × S | 6.9 | −14 | 2 × S | 6.9 | −12 | 2 × G | 7.6 | −7 | 2 × G | 7.6 | −7 |

| | α-HNN | H74 | H58 | H20 |
|---|---|---|---|---|
| $R$(C···O) | 3.38 | 2.99 | 2.82 | 3.02 |
| H···O—N | 112 | 115 | 114 | 109 |
| C—H···O | 160 | 156 | 164 | 161 |
| $R$(H···O) | 2.34 | 1.98 | 1.76 | 1.98 |

† Energies calculated with SET2 parameters.

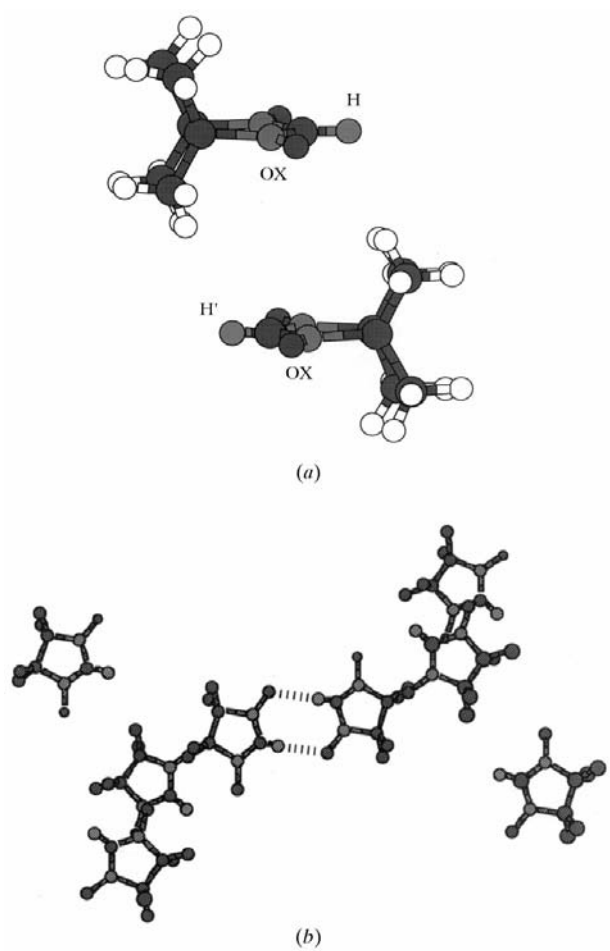


Fig. 3. Nearest-neighbour molecules in β-HNN. (*a*) DIM1 dimer, H···H′ 5.08, OX···OX 4.97 Å. (*b*) An HB dimer with some surrounding molecules.

## 4. Computer generation of polymorphs: results

A systematic computational generation of possible polymorphs (Gavezzotti & Filippini, 1995) for HNN was undertaken, as mentioned above, using the *PROMET* procedure. The molecular volume of the HNN molecule is 149 Å$^3$, and, assuming a packing coefficient of 0.7, a cell volume of 213 Å$^3$ per molecule is to be expected, with a density of 1.22 g cm$^{-3}$. The expected (Gavezzotti, 1994) dispersive lattice energy is $0.84Z + 39 = 92$ kJ mol$^{-1}$ (where $Z$ is the number of valence electrons in the molecule). The experimental crystal structure has $V_{cell}$ = 211.4 Å$^3$, density 1.233 g cm$^{-3}$, while the SET1 calculated lattice energy is 88 kJ mol$^{-1}$. These results demonstrate the usefulness of statistical correlations in the prediction of relevant crystal properties and as guidelines in crystal-structure generation and prediction.

### 4.1. *SET1 results*

The *PROMET* search in seven space groups ($P1$, $P\bar{1}$, $P2_1$, $P2_1/c$, $P2_12_12_1$, $Pca2_1$, $Pna2_1$) yielded about 3600 crystal structures. A first screening procedure, discarding duplicate cells and accepting – as in previous experience – structures with a cohesive energy of ∼75% of the expected energy (see above), extracted 214 structures with a lattice packing energy PE < −71 kJ mol$^{-1}$ (that is, more cohesive than 71 kJ mol$^{-1}$). Further checks with machine and manual recognition of similar structures resulted in the independent structures listed in Table 3.

Pure translation in space group $P1$, without hydrogen bonding, produces an acceptable crystal structure (Fig. 4) with a density less than 2% lower and a PE just 7% higher than that of the most cohesive one. That it is indeed a stable structure is demonstrated by the fact that

Table 3. *SET1 calculations, crystal structures generated by PROMET*

Cell parameters are in Å and °, densities are in g cm$^{-3}$, energies are in kJ mol$^{-1}$, distances are in Å. Each structure determinant comprises a symmetry operator symbol (I inversion centre, S screw, G glide, T translation), a distance between centres of mass and an interaction energy.

| | *a* | *b* | *c* | $\alpha$ | $\beta$ | $\gamma$ | Density | PE | H···O | Label | First structure determinant | | |
|---|---|---|---|---|---|---|---|---|---|---|---|---|---|
| $P1$ | 5.91 | 6.04 | 6.59 | 103 | 109 | 106 | 1.28 | −77.8 | — | H1 | T | 5.9 | −15 |
| $P\bar{1}$ | 5.99 | 6.60 | 11.36 | 74 | 75 | 70 | 1.30 | −83.6 | 1.92 | H4 | I | 5.4 | −21 |
| | 6.27 | 6.50 | 11.04 | 76 | 85 | 69 | 1.27 | −80.8 | 1.98 | H2 | I | 5.1 | −26 |
| $P2_1$ | 7.19 | 8.55 | 6.67 | — | 102 | — | 1.30 | −81.6 | 2.15 | H5 | S | 6.1 | −15 |
| $P2_1/c$ | 6.23 | 10.91 | 12.32 | — | 106 | — | 1.30 | −84.9 | 1.98 | H20 | I | 5.1 | −25 |
| | 7.41 | 10.54 | 11.33 | — | 113 | — | 1.28 | −82.8 | 1.93 | H9 | G | 5.8 | −19 |
| | 8.42 | 7.83 | 12.58 | — | 99 | — | 1.27 | −81.6 | 1.93 | H8 | I | 5.7 | −21 |
| | 11.82 | 6.12 | 11.21 | — | 95 | — | 1.29 | −80.8 | 2.00 | H7 | G | 5.9 | −16 |
| | 10.06† | 11.67 | 6.93 | — | 95 | — | 1.29 | −80.3 | 2.36‡ | H12 | I | 5.2 | −23 |
| $P2_12_12_1$ | 7.73 | 9.47 | 11.05 | — | — | — | 1.29 | −80.8 | 2.05 | H17 | S | 5.1 | −24 |
| $Pca2_1$ | 11.11 | 8.99 | 8.21 | — | — | — | 1.27 | −79.5 | 1.94 | H18 | S | 6.0 | −15 |
| $Pna2_1$ | 7.14 | 10.54 | 10.92 | — | — | — | 1.27 | −78.7 | 1.93 | H19 | G | 5.7 | −22 |

† $P2_1/n$. ‡ Second hydrogen bond 2.15 Å.

its calculated lattice vibration frequencies (Filippini & Gramaccioli, 1986) are real and reasonable (62–119 cm$^{-1}$). Centrosymmetry in space group $P\bar{1}$ produces some very stable crystal structures, as is usually the case for molecules of complex shape. Lattice vibration frequencies span a wider range (*e.g.* 47–128 cm$^{-1}$ for H4) as appropriate for the higher number of molecules in the cell; however, all lattice vibration frequencies for *PROMET*-generated structures are within the range 30–130 cm$^{-1}$, quite usual for organic molecules. This is no doubt the result of the rather stringent optimization requirements of the *PCK* procedure, which ensures a positive-definite Hessian and a real minimum in the energy hypersurface (subject to space-group constraints).

A wide choice of $P2_1/c$ crystal structures is produced by SET1 potentials, the unique-axis length varying from 6.12 to 10.91 Å within a 4 kJ mol$^{-1}$ energy range. The $\alpha$-phase structure appears among them (structure H20). Non-centrosymmetric crystal structures are calculated to have lower densities and higher packing energies; when potentials without charges are used, these two quantities show, as expected, a rather strict inverse proportionality.

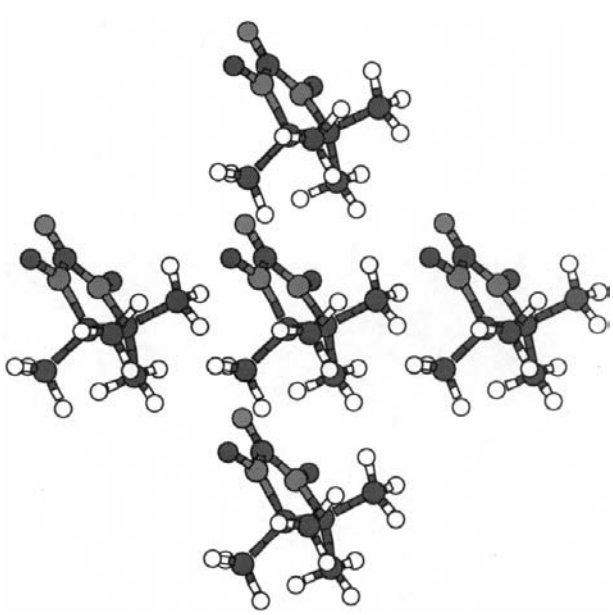

Fig. 4. Crystal structure H1 in space group $P1$ (no hydrogen bonds).

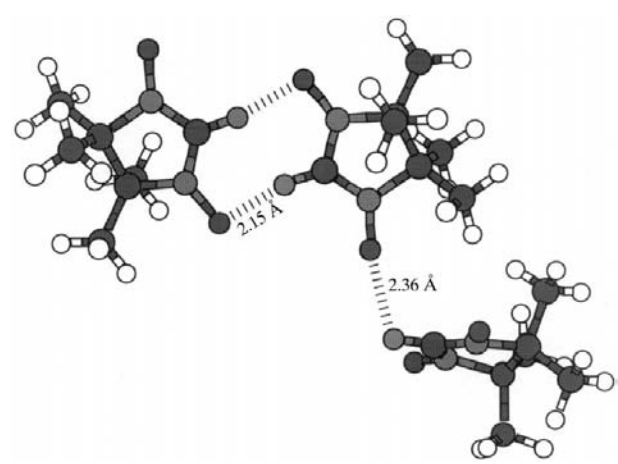


Fig. 5. An unusual bifurcated hydrogen-bonding scheme in crystal structure H12.

Table 4. *SET1Q calculations, crystal structures generated by PROMET*

Details as for Table 3.

| | *a* | *b* | *c* | $\alpha$ | $\beta$ | $\gamma$ | Density | PE | Label | H···O | First structure determinant | | |
|---|---|---|---|---|---|---|---|---|---|---|---|---|---|
| $P\bar{1}$ | 5.97 | 6.22 | 11.62 | 78 | 79 | 72 | 1.31 | −128.9 | H54 | 1.77 | I | 5.8 | −20 |
| | 6.01 | 6.73 | 11.05 | 86 | 82 | 69 | 1.26 | −123.4 | H51 | 1.77 | I | 5.6 | −18 |
| $P2_1$ | 6.22 | 7.77 | 8.47 | | 95 | | 1.28 | −120.5 | H63 | 1.82 | S | 6.1 | −15 |
| $P2_1/c$ | 7.16 | 10.42 | 11.48 | | 112 | | 1.31 | −128.0 | H59 | 1.79 | I | 5.7 | −19 |
| | 6.26 | 10.89 | 12.10 | | 105 | | 1.31 | −127.2 | H58 | 1.76 | I | 5.1 | −25 |
| | 5.90 | 10.49 | 16.22 | | 124 | | 1.26 | −125.9 | H62 | 1.75 | I | 5.8 | −20 |
| | 10.67 | 6.79 | 11.56 | | 98 | | 1.26 | −125.5 | H52 | 1.75 | I | 5.6 | −23 |
| | 11.17 | 6.83 | 12.06 | | 120 | | 1.30 | −125.1 | H57 | 1.80 | G | 6.0 | −16 |
| | 8.44 | 7.68 | 12.59 | | 100 | | 1.30 | −123.8 | H56 | 1.78 | I | 5.7 | −21 |
| $P2_12_12_1$ | 16.63 | 6.26 | 7.79 | | | | 1.29 | −122.2 | H53 | 1.80 | S | 6.1 | −15 |

Hydrogen-bonding distances are all predicted too short with respect to experiment, owing to the very short equilibrium distance in the potential energy curve. While nearly all centrosymmetric crystal structures contain the $R_8^{2,2}$ ring, structure H12 (Fig. 5) displays an interesting bifurcated hydrogen-bonding pattern.

A proper crystal-structure prediction depends, to a first approximation, on ranking the lattice energies and sorting out the most stable one. Actually, the intrinsic energetic resolution of the whole procedure can be estimated to be around 4–8 kJ mol$^{-1}$ (Gavezzotti, 1994), and, as expected from wide experience (Gavezzotti, 1996; van Eijck *et al.*, 1995; Mooij *et al.*, 1998; Gavezzotti & Filippini, 1998), about ten crystal structures for HNN are found within this range, demonstrating that crystal-structure prediction based on energy criteria alone is impossible. This is apparent from the SET1 data in Table 3, but remains true whatever the potential employed. Besides, the energetic similarity among polymorphic organic crystal structures is borne out also by an analysis of experimental data (Gavezzotti, 1991). Thus, we do not attach a high significance to the apparently encouraging result that the observed crystal structure is marginally more stable than the others.

### 4.2. *SET1Q results*

Only four space groups were considered in this case and the data are collected in Table 4. The results are, in a general sense, quite similar to the SET1 results: the most stable structure in $P\bar{1}$, H54, is nearly identical to structure H4. The X-ray structure is now retrieved as structure H58, marginally (not significantly) less stable than structure H59, a modulation with a shorter unique axis, shorter glide direction and a longer translation. The set of $P2_1/c$ structures with drastically shorter (7 *vs* 11 Å)

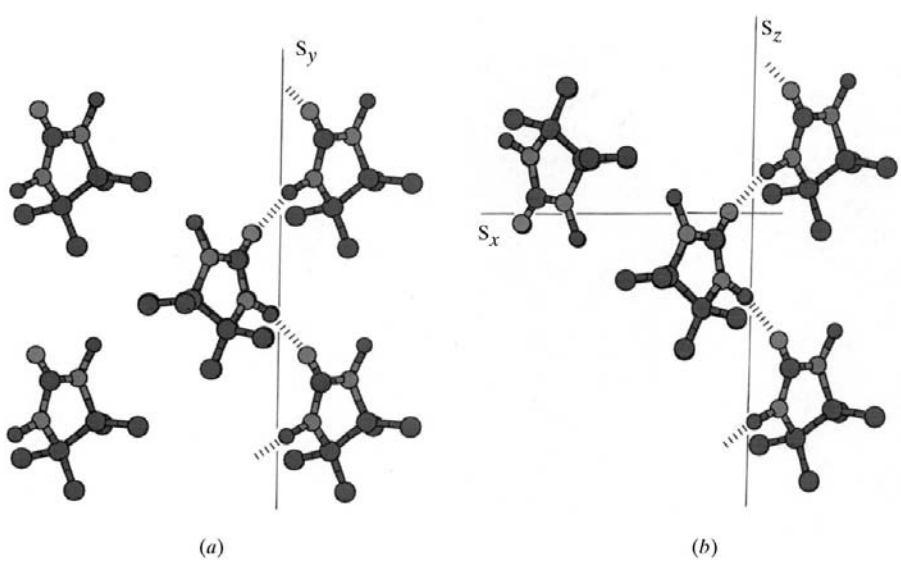


Fig. 6. Catemer motifs in (*a*) structure H63, and (*b*) structure H53. The molecular ribbons along the screw axes are nearly identical.

unique axes appears in this case too. The only noticeable effect of the introduction of charges seems to be a shortening of the hydrogen-bonding distance to about 1.8 Å; a negative result considering that the observed distance is 2.34 Å. This is probably a consequence of the increased attractive power of Coulomb-type potential contributions.

Fig. 6 shows two stable catemer structures obtained in the non-centrosymmetric space groups. In both cases the direction of the hydrogen-bonding chain is along an 8 Å screw axis ($S_y$ in $P2_1$, $S_z$ in $P2_12_12_1$).

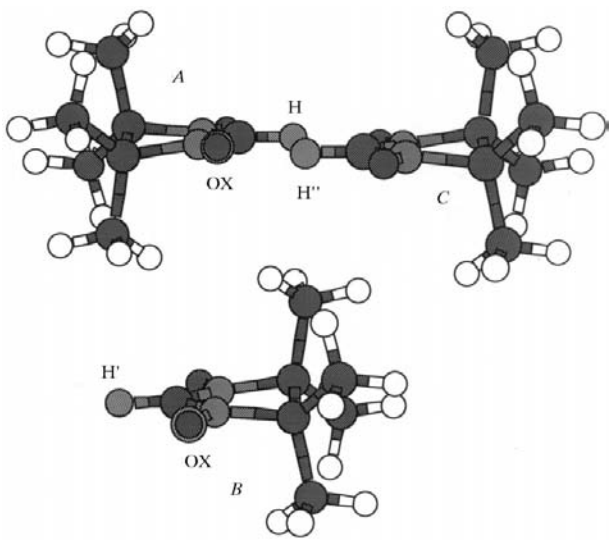


Fig. 7. Main structure determinants in crystal structure H72, $P\bar{1}$; compare with Fig. 3, $P2_1/c$. H···H′ 6.46, H′···H″ 5.97, OX···OX 5.58 Å.

### 4.3. *SET2Q results*

Only the two centrosymmetric space groups were considered in this case. The $P\bar{1}$ results are quite similar to those with other potential parameter sets: the $P\bar{1}$ crystal structure H72 (similar to H4 and H54) includes the two basic building blocks of the X-ray structure, namely the DIM1 and HB dimers (Fig. 7), and is accordingly about as stable as the observed $P2_1/c$ structure.

Structure H74 reproduces the X-ray structure best (Fig. 2), including the exact ordering in the structure determinant (Table 2). The hydrogen-bond distances are longer than in the SET1Q results, but still appreciably shorter than the observed ones. Apparently, structure H74 ranks rather low in energy; however, closer scrutiny revealed that the final optimization stage in *PROMET* had stopped after reaching the maximum number of cycles allowed, rather than at true convergence. Restarting the minimization procedure resulted in cell parameters and an energy practically indentical to those shown in Table 1 for SET2Q. Such technical faults may

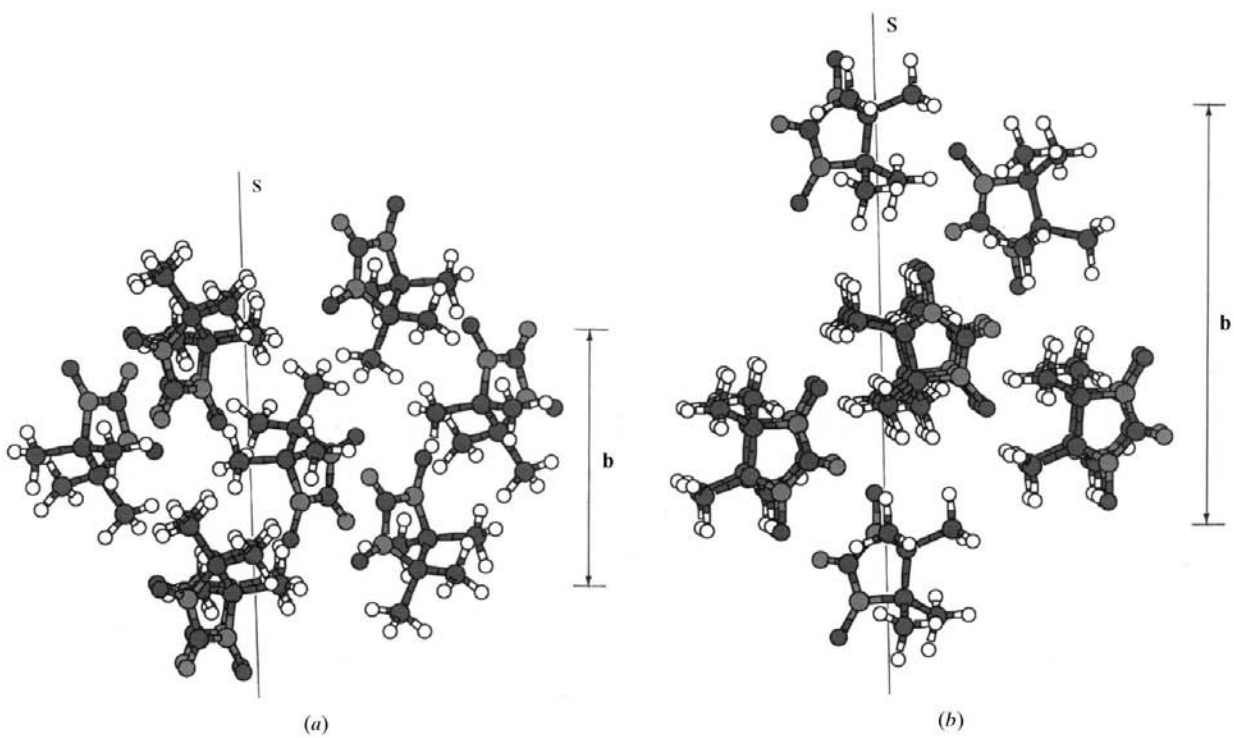


Fig. 8. Crystal structures (*a*) H73 and (*b*) H78, $P2_1/c$: molecular arrangements along the unique *b* axis.

be unavoidable whenever a very large number of optimizations are performed, in which different convergence thresholds would be needed for different cases but uniform parameters are chosen as a compromise between accuracy and speed. This example illustrates how technical factors can influence the energy ordering in an unpredictable way.

Finally, Fig. 8 shows how a compact crystal packing can be reached in the same space group, $P2_1/c$, with widely different values of the unique axis lengths. In structure H73, the molecular centre of mass is rather far from the screw axis and molecules may pile up along $y$ with a relatively short screw translation. In structure H78, the centre of mass stays close to the screw axis and the displacement must accordingly be longer. The packing energies, including Coulombic contributions, are not significantly different. Such examples further demonstrate how crystal stability can be achieved over a very wide range of three-dimensional arrangements of molecules of complex shape.

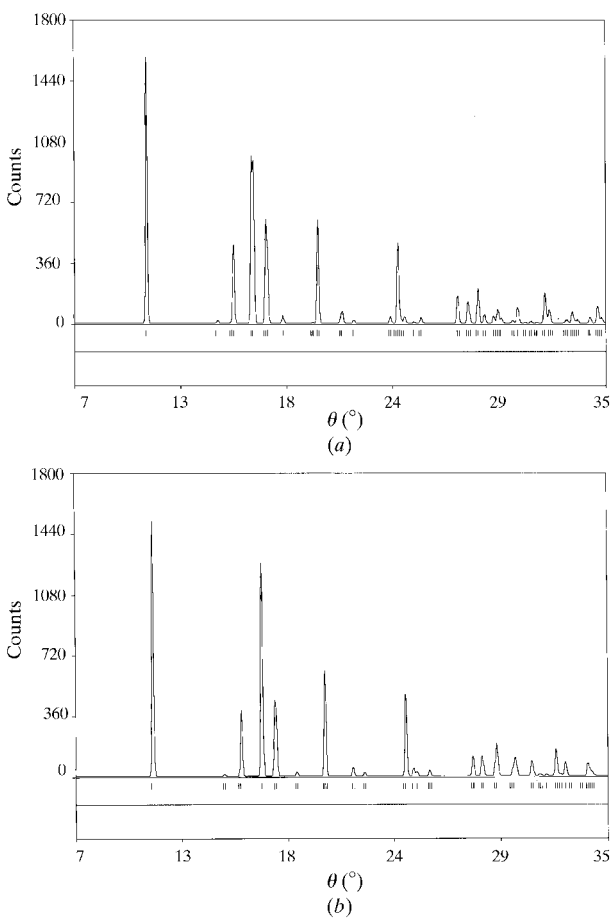


Fig. 9. Powder patterns generated from single-crystal atomic coordinates (Cu $K\alpha$ radiation, $B$ = 4 Å$^2$ for all atoms): (*a*) $\alpha$-HNN, X-ray structure, and (*b*) the same after *PCK* relaxation, SET2Q parameters..

## 5. Discussion

Comparison of crystal structures can be carried out using powder patterns generated from the atomic coordinates, either from single-crystal X-ray refinement or from *PROMET* generation. Fig. 9 shows a comparison between the pattern for the $\alpha$ polymorph from X-ray refinement (Fig. 9*a*) and after relaxation under the SET2Q potential (Fig. 9*b*). Aside from minor shifts in $\theta$, owing to subtle changes in cell dimensions, the two patterns are almost indistinguishable. Fig. 10 compares the powder patterns from the computational polymorphs best resembling the observed $\alpha$ polymorph (H74, H58 and H20). All three patterns coincide in the most prominent feature at $\theta = 11°$, and even the 15–18° region is very similar in all of them. The pattern for the SET2Q result for H74 is, however, the one which resembles the experimental pattern most in terms of the features (especially the intensity ratios) in the 18–26° region. Beyond that, agreement depends on somewhat subjective judgement.

Fig. 11 shows some packing diagrams. Although projections, especially in non-orthogonal cells, may be very deceiving, the similarity of the calculated and experimental crystal structures can be clearly appreciated. As already emphasized, however, the results presented in Tables 3–5 would not have allowed a truly *de novo*, independent crystal-structure prediction on the basis of the energy criterion alone, in the absence of diffraction data, because the observed structure is not the most stable one. The availability of the powder pattern of Fig. 9(*a*), or the cell parameters and the space group, would have allowed an unequivocal identification of the observed crystal structure. The comparison of powder spectra showed that any crystal structure among H74, H58 and H20 would have represented a successful solution of the phase problem.

Another main result of our calculations, not really new, is that many almost isoenergetic molecular arrangements are compatible with close packing. The analyses of molecular build-ups presented here in various packing diagrams emphasizes again, if need be, the extremely multiform character of molecular recognition, where many (a great many) minima in phase space are separated by extremely low energy differences and, almost certainly, by extremely high interconversion barriers owing to the necessity of breaking apart the starting lattice before converging to the new one. This is the analogue of conformational flexibility in large isolated molecules (although conversion barriers may be very low there), and is not really surprising if one considers the high dimensionality of the lattice-energy landscape. As a consequence, our results further corroborate the conclusion that even using complex computational procedures, supported by potential energy calculations based on accurate physicochemical data, *a true crystal-structure prediction from molecular structure*

*alone is possible only if auxiliary diffraction data (typically, cell parameters or a powder pattern) are available* (Gavezzotti & Filippini, 1996).

The other main result, for the moment pertinent only to this particular crystal structure, but the generality of which it would be important to assess, is that the computational procedure is able to spot and reconstruct the observed crystal structure of such a polar compound

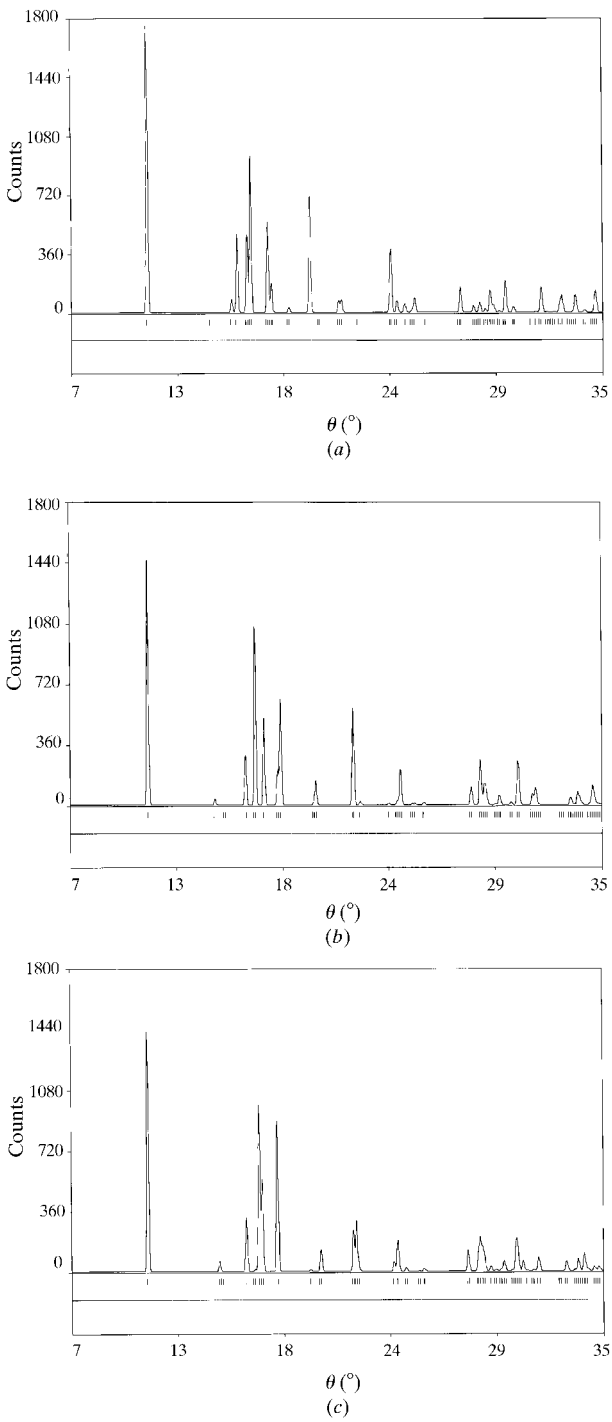


Fig. 10. Powder patterns generated (as in Fig. 9) for (*a*) structure H74, (*b*) structure H58 and (*c*) structure H20.

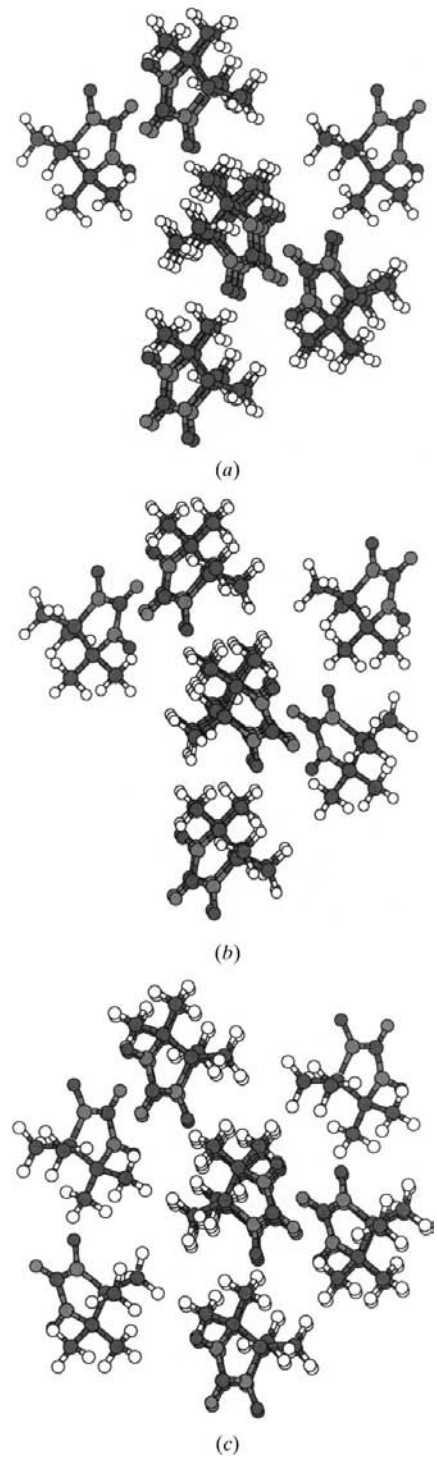


Fig. 11. Packing diagrams for α-HNN; (*a*) X-ray structure, (*b*) structure H74 and (*c*) structure H20.

Table 5. *SET2Q calculations, crystal structures generated by PROMET*

Details as for Table 3. Note: H4 = H54 = H72, H59 = H75, H20 = H58 = H74 = X-ray, H8 = H56 = H73.

| | | | | | | | | | | | First structure determinant | | |
|---|---|---|---|---|---|---|---|---|---|---|---|---|---|
| | *a* | *b* | *c* | $\alpha$ | $\beta$ | $\gamma$ | Density | PE | Label | H···O | | | |
| $P\bar{1}$ | 5.97 | 6.18 | 11.80 | 78 | 78 | 71 | 1.30 | −122.6 | H72 | 1.95 | I | 5.9 | −19 |
| | 6.17 | 6.39 | 11.58 | 94 | 103 | 115 | 1.31 | −120.0 | H71 | 1.95 | I | 5.5 | −21 |
| $P2_1/c$ | 5.86 | 13.49 | 12.10 | | 124 | | 1.31 | −125.1 | H78 | 1.96 | I | 5.7 | −20 |
| | 7.16 | 10.39 | 11.62 | | 112 | | 1.30 | −122.2 | H75 | 1.97 | I | 5.7 | −19 |
| | 8.17 | 10.30 | 11.34 | | 124 | | 1.32 | −119.2 | H76 | 2.02 | G | 5.8 | −16 |
| | 6.38 | 11.45 | 11.61 | | 104 | | 1.27 | −118.0 | H74 | 1.98 | I | 5.1 | −26 |
| | 8.49 | 7.74 | 12.57 | | 100 | | 1.28 | −117.6 | H73 | 1.95 | I | 5.7 | −21 |
| | 6.06 | 12.40 | 11.95 | | 114 | | 1.28 | −117.2 | H77 | 1.96 | T | 6.1 | −14 |

even without introducing Coulomb-type terms in the potential field. SET2Q calculations demonstrate that the Coulombic contribution to the total lattice energy is highly stabilizing, being of the order of 30% of the total lattice energy, although a definite quantitative appreciation would require a more sophisticated force field. Yet, SET1 potentials, which do incorporate a certain amount of Coulombic interaction, as explicitly allowed during their calibration, although they are certainly not expected to reproduce all of it, can steer the computational procedure to the observed polymorph almost as efficiently as potential sets including $R^{-1}$ terms. The only advantage found with the introduction of Coulomb-type terms was a quicker approach to the solution (a finer grid was used in SET1 calculations) and a somewhat more precise determination (see Table 2 and Fig. 10). The cost is an increase in computing effort, owing to the need to estimate charges by quantum-chemical methods and to the problem of convergence of $R^{-1}$ summations.

Consistent progress has been made recently in the efficiency of computer procedures for crystal-structure generation, and computer-aided crystal-structure simulation is by now a very helpful tool for the solid-state chemist. However, empirical force fields have an inherent inaccuracy which cannot be overcome by calibration, and even more sophisticated force fields cannot reach a final predictive robustness; having many structures of similar energy shows that enthalpic factors are not enough. A more careful consideration of entropic and kinetic factors, by means so far still to be discovered, will clearly be needed before a consistent protocol for prediction and control of crystal structures can be devised.

## References


Bates, J. B. & Busing, W. R. (1974). *J. Chem. Phys*. **60**, 2414–2419.

Besler, B. H., Merz, K. M. Jr & Kollman, P. A. (1990). *J. Comput. Chem*. **11**, 431–439.

Bürgi, H. B., Dunitz, J. D. & Shefter, E. (1974). *Acta Cryst*. B**30**, 1517–1527.

Deumal, M., Cirujeda, J., Veciana, J., Kinoshita, M., Hosokoshi, Y. & Novoa, J. J. (1997). *Chem. Phys. Lett*. **265**, 190–199.

Eijck, B. P. van, Mooij, W. T. M. & Kroon, J. (1995). *Acta Cryst*. B**51**, 99–103.

Filippini, G. & Gavezzotti, A. (1993). *Acta Cryst*. B**49**, 868–880.

Filippini, G. & Gavezzotti, A. (1994). *Chem. Phys. Lett*. **231**, 86–92.

Filippini, G. & Gramaccioli, C. M. (1986). *Acta Cryst*. B**42**, 605–609.

Frisch, M. J., Trucks, G. W., Schlegel, H. B., Gill, P. M. W., Johnson, B. G., Robb, M. A., Cheeseman, J. R., Keith, T., Petersson, G. A., Montgomery, J. A., Raghavachari, K., Al-Laham, M. A., Zakrzewski, V. G., Ortiz, J. V., Foresman, J. B., Cioslowski, J., Stefanov, B. B., Nanayakkara, A., Challacombe, M., Peng, C. Y., Ayala, P. Y., Chen, W., Wong, M. W., Andres, J. L., Replogle, E. S., Gomperts, R., Martin, R. L., Fox, D. J., Binkley, J. S., Defrees, D. J., Baker, J., Stewart, J. P., Head-Gordon, M., Gonzalez, C. & Pople, J. A. (1995). *GAUSSIAN*94. Revision C3. Gaussian Inc., Pittsburgh, Pennsylvania, USA.

Gatteschi, D., Kahn, O., Miller, J. S. & Palacio, F. (1991). Editors. *Molecular Magnetic Materials*. Dordrecht: Kluwer Academic Publishers.

Gavezzotti, A. (1991). *J. Phys. Chem.* **95**, 8948–8955.

Gavezzotti, A. (1994). *Acc. Chem. Res*. **27**, 309–314.

Gavezzotti, A. (1996). *Acta Cryst*. B**52**, 201–208.

Gavezzotti, A. (1997). *PROMET*5.3. *A Program for the Generation of Possible Crystal Structures from the Molecular Structure of Organic Compounds*. University of Milan, Italy.

Gavezzotti, A. & Filippini, G. (1994). *J. Phys. Chem*. **98**, 4831–4837.

Gavezzotti, A. & Filippini, G. (1995). *J. Am. Chem. Soc*. **117**, 12299–12305.

Gavezzotti, A. & Filippini, G. (1996). *J. Am. Chem. Soc*. **118**, 7153–7157.

Gavezzotti, A. & Filippini, G. (1998). *J. Chem. Soc. Chem. Commun*. pp. 287–294.

Hosokoshi, Y. (1995). PhD thesis, University of Tokyo, Japan.

Hosokoshi, Y., Tamura, M., Nozawa, K., Suzuki, S., Kinoshita, M., Sawa, H. & Kato, R. (1995). *Synth. Met*. **71**, 1795–1796.

Hosokoshi, Y., Tamura, M., Nozawa, K., Suzuki, S., Sawa, H., Kato, R. & Kinoshita, M. (1995). *Mol. Cryst. Liq. Cryst*. **271**, 115–122.

Itoh, K., Miller, J. S. & Taku, T. (1997). Editors. *Mol. Cryst. Liq. Cryst*. **305**–**306**.
Kahn, O. (1993). *Molecular Magnetism*. New York: VCH.
Kinoshita, M. (1994). *Jpn. J. Appl. Phys*. **33**, 5718–5733.
Miller, J. S. & Epstein, A. J. (1994). *Angew. Chem. Int. Ed. Engl*. **33**, 385–415.
Mooij, W. T. M., van Eijck, B. P., Price, S., Verwer, P. & Kroon, J. (1998). *J. Comput. Chem*. **19**, 459–474.
Novoa, J. J. & Deumal, M. (1997). *Mol. Cryst. Liq. Cryst*. **305**, 143–156.
Takeda, K., Mito, M., Kawae, T., Takumi, M., Nagata, K., Tamura, M. & Kinoshita, M. (1998). *J. Phys. Chem. B*, **102**, 671–676.
Williams, D. E. (1983). *PCK*83. QCPE Program 548. Quantum Chemistry Program Exchange, Chemistry Department, Indiana University, Bloomington, Indiana, USA.